Size independence of UHPC ductility

E. Chuang & F.J. Ulm
Massachusetts Institute of Technology, Cambridge, Massachusetts, U.S.A.

ABSTRACT: This paper examines the size effects in UHPC tensile behavior. It is shown that while the first cracking strength of UHPC is indeed size dependent, the post-cracking behavior is not only ductile, but also size independent. This behavior is displayed with an experimental examination of UHPC beams ranging from 70 mm to 910 mm in height.

Keywords: high performance concrete, size effects, ductility.

1 INTRODUCTION

Breakthroughs in the material science of cementitious materials have led to the development of fiber reinforced ultra high performance concretes (UHPC), which have encouraged engineers to reevaluate the application of cementitious materials in civil engineering structures. For example, these materials could enable the elimination of shear stirrups in the next generation of large-scale girders (Park et al., 2003). Regardless of the magnitude of the tensile strengths of UHPC materials, the key to safe application of these materials in unreinforced tension and shear is their ductile behavior. However, the size dependent behavior of cementitious materials (Bazant & Planas, 1998) may undermine the structural reliability of UHPC ductility. To this end, an experimental study, which exhibits the size independence of UHPC ductility, is presented.

In the first part of this paper, a previously presented UHPC model and corresponding finite element (FE) implementation is reviewed. The UHPC model is a two-phase model, one phase representing the cementitious matrix and the other representing the reinforcing fibers (Chuang & Ulm, 2002b, Chuang & Ulm, 2003). The finite element implementation of the model was shown to provide reliable and relevant predictions of load-deflection behavior, local strain behavior, and cracking behavior for two structural case studies: a flexural girder and a shear girder which have been recently tested by the FHWA (Chuang et al., 2003).

In the second part of this paper, an experimental examination of small scale UHPC beam is developed. The UHPC constitutive model and corresponding finite element implementation offer tools for obtaining the structurally dependent material behavior from experimental results. More specifically, through inverse analysis, the finite element implementation can yield the material parameters which describe a particular structural behavior. In particular, three ductility metrics are shown to be size independent:

1. The stiffness ratio: the ratio of post-cracking stiffness to the initial linear elastic stiffness.

2. The ductility ratio: the ratio of UHPC residual strength immediately following first cracking to the strength drop during cracking.

3. The peak tensile (yield) strength.

In this way, the size independence of UHPC ductility is confirmed. It is on the basis of this size independence that the ductile strength of UHPC can be utilized safely.
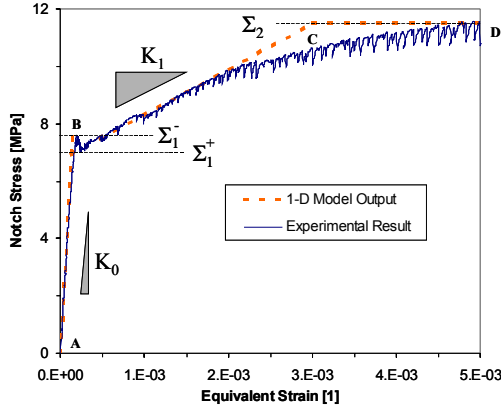
Figure 1. Tensile stress-strain curve for a UHPC specimen (data from Lafarge) and corresponding 1-D UHPC model.

2 UHPC MATERIAL MODEL AND INPUT PARAMETERS

Figure 1 displays the typical material response of UHPC materials obtained from a displacement driven notched tensile plate test. The UHPC behaves elastically with a stiffness of K_0 from A to B in Figure 1. At this stage, the cementitious matrix phase carries most of the tensile load.

At point B, the UHPC reaches its virgin tensile strength Σ_1^- and exhibits a brittle strength drop to a post-cracking strength Σ_1^+. This is generally associated with the propagation of microcracks. Having introduced significant cracking into the matrix, the composite material exhibits a decrease in stiffness (secant stiffness K_1) during the next stage of loading, B to C. At point C, the UHPC reaches its maximum post-cracking strength Σ_2. While the application of the tensile strength of cementitious materials is often restricted by the uncertainty regarding their tensile values, careful batching and mixing procedures for UHPC results in less dispersive tensile values, allowing safe exploitation of the tensile and shear capacity of UHPC in structural applications.

To capture this physically observed UHPC macroscopic behavior, a two-phase model, which is displayed in Figure 2, is employed. This model was formulated not only to capture physically observed macroscopic behavior, but also micromechanical processes (such as elasticity, cracking, and yielding) which occur at a scale below. In this

model, developed in detail by Chuang and Ulm (2002a), a brittle-plastic composite matrix phase (stiffness C_M, brittle strength f_t, plastic strength k_y) is coupled to an elasto-plastic composite fiber phase (stiffness C_F, strength f_y) by means of a composite interface spring (stiffness M). This composite interface spring is not activated until cracking occurs in the composite matrix phase. Figure 1 compares the stress-strain response of the 1-D model with the experimentally determined UHPC stress-strain relation. Table 1 displays the determined model parameter values suggested by the experimental data given in Figure 1.
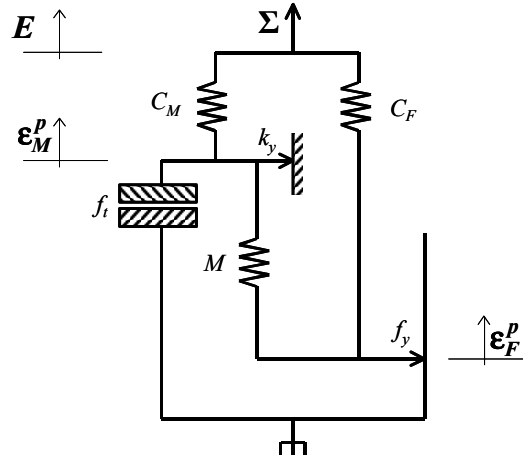

Figure 2: The 1-D UHPC model.

Table 1: UHPC model parameters and corresponding values for DUCTAL[TM] UHPC

Model Parameter	Description	DUCTAL[TM] Value
C_M [GPa]	Stiffness of the composite matrix	53.9
C_F [Gpa]	Stiffness of the composite fiber	0
M [GPa]	Stiffness of the composite interface	1.65
f_t [MPa]	Brittle tensile strength of the composite matrix	0.7
k_y [MPa]	Post-cracking tensile strength of the composite matrix	6.9
f_y [MPa]	Tensile strength of the composite fiber	4.6

3   VALIDATION OF THE UHPC MODEL

To validate the UHPC model and its finite element implementation, two tests performed by the FHWA were investigated (FHWA, 2002). [For the complete validation of the UHPC model, refer to Chuang et al. (2003).] Both tests involved AASHTO Type II beams, 910 mm in height, comprised of DUCTAL^{TM} without shear reinforcement:

- FHWA flexure test. A prestressed girder with a 23.9 m long test span was loaded in four point bending with two equal load points (total load P) located 0.9 m from the midspan (see Figure 3 (Top)).
- FHWA shear test. A 4.3 m girder was tested in three point bending. The load P was applied off-center, 1.8 m from one of the supports, in order to induce high shear stresses in the short load span (see Figure 3 (Bottom)).
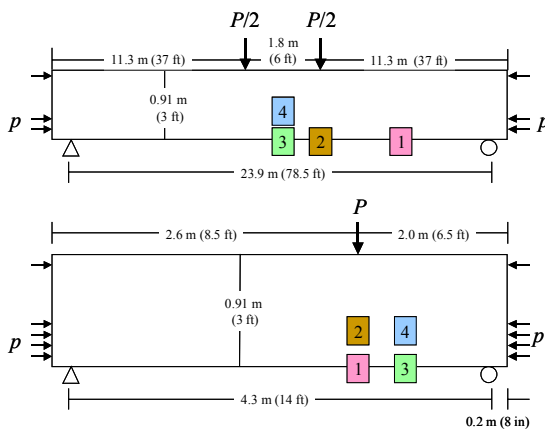

Figure 3: Loading configuration and strain gauge location for: (Top) the FHWA flexure test; (Bottom) the FHWA shear test.

The FHWA tests were numerically simulated to gauge the accuracy and reliability of the UHPC model. The finite element simulation was validated with the experimental data with respect to three different criteria:

- Load-deflection curves. The load-deflection curves of the FHWA specimen and the FE simulation demonstrated very good correlation as shown in Figure 4.

- Strain gauge measurements. The FE program provides results for the deflection of the nodes in a given mesh during loading. Strain results are calculated as the change in distance between two nodes divided by the original distance between the nodes. Strain predictions obtained from the FE simulation exhibited excellent agreement with strain measurements from strain gauges placed at various locations on the FHWA specimens.

- Cracking patterns. Plastic strains in the composite matrix can be related to cracking, which occurs in the cementititous matrix of UHPC. The composite matrix plastic strains as given by the FE simulation accurately modeled cracking observed in the FHWA specimens.
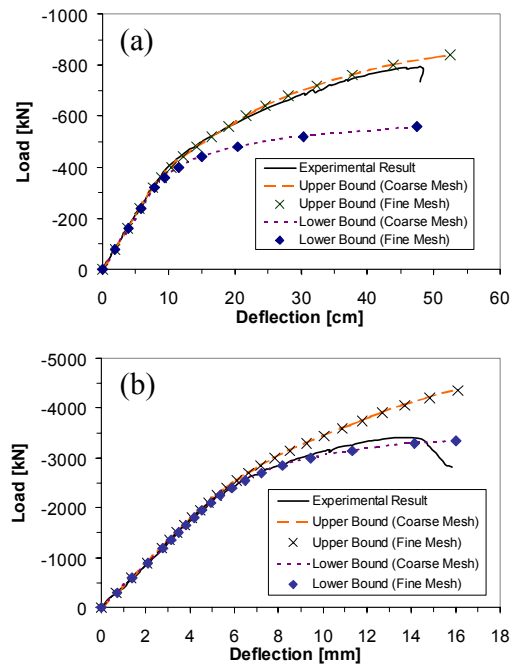

Figure 4: Load-deflection results from the FHWA simulations: (a) the FHWA flexure test; (b) the FHWA shear test.

In this way, the UHPC model was shown to appropriately predict the behavior of UHPC structures not only at the global level, i.e. load-

deflection behavior, but also the local level, i.e. strain and cracking results. Furthermore, the suitability of the UHPC model parameters, as derived from a notched tensile plate test, for describing UHPC material behavior in large scale structures is exemplified.

4 SIZE EFFECT IN UHPC STRUCTURES

The last part of this paper is devoted to the study of size effects which influence the UHPC model parameters. Size effects detected in cementitious structures can be traced back to fracture mechanics sources. In particular, for a given cementitious material, a fracture process zone of constant length (a material parameter) forms in front of any crack. The fracture process zone has a much more significant crack blunting effect on smaller sized structures than larger structures (Bažant & Planas, 1998). For this reason, the first cracking strengths of UHPC materials Σ_1^- (see Figure 1) is expected to exhibit higher values in smaller structures than larger structures.

Using micromechanical theory, the size effect in the UHPC model parameters related to first cracking, f_t and k_y, was revealed by Chuang & Ulm (2002b). However, their relative proportion, termed the ductility ratio $R_D = k_y/f_t$, was shown to be size independent. In this section, this finding is validated at a structural level. Two small scale case studies are examined: an unnotched beam and two self-similar notched beams. For both loading cases, size effects on the first cracking strength $\Sigma_1^- = k_y + f_t$ and the post-cracking strength $\Sigma_1^+ \approx k_y$ are elucidated through model-based simulations. However, the size independence of UHPC ductility is also displayed for both cases. More precisely, the yield strength of UHPC, $\Sigma_2 = k_y + f_y$, is effectively shown to be size independent, a characteristic property of UHPC that allows for secure application of the material in structures.

4.1 Case study: a small scale unnotched beam

Figure 5(a) shows the load-deflection response of a small scale UHPC beam loaded in four point bending (SS4P) (test performed by Lafarge). The prismatic beam loaded in four point bending with three equal spans, had a total test span of L = 210 mm, a height of h = 70 mm, and a width of b = 70 mm. Also shown in Figure 5(a) is the FE simulation of SS4P using the DUCTAL^{TM} material parameters listed in Table 2 ("Original" values). With the "Original" values, which appropriately characterize the large scale behavior, the FE solution significantly underestimates the actual behavior of the beam. The divergence between the two load-deflection curves begins at the onset of plasticity in the FE simulation, which is indicative of the underestimation of the first cracking strength. Thus, in this example, a size effect becomes apparent.
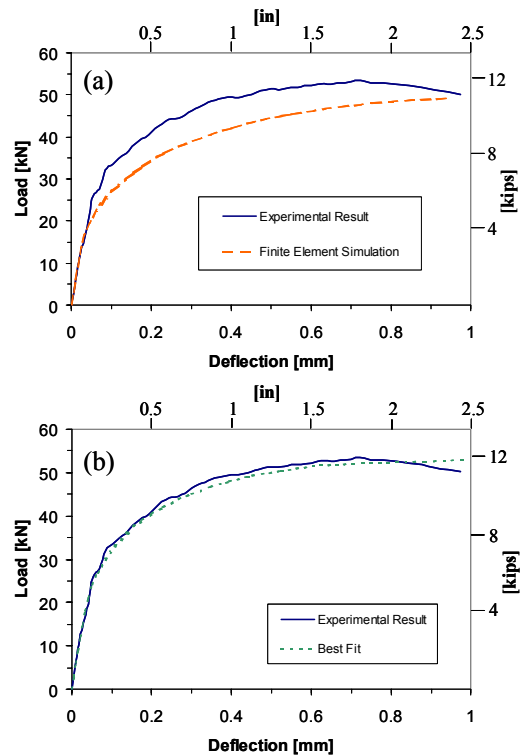

Figure 5: Load-deflection behavior for SS4P determined experimentally and with FE simulation for (a) "Original" material parameters and (b) "Best Fit" material parameters.

Table 2: "Best Fit" macroscopic behavior listed with related model parameters and ductility parameters for the small scale tests as determined by inverse analysis.

Tensile Value	Original	Best Fit		
		SS4P	N70	N100
Σ_1^- (MPa)	7.6	10.5	10	9.5
Σ_1^+ (MPa)	6.9	9.6	9.1	8.7
Σ_2 (MPa)	11.5	12.5	11.5	11.5
Model Value				
f_t (MPa)	0.7	0.95	0.91	0.86
k_y (MPa)	6.9	9.55	9.1	8.64
f_y (MPa)	4.6	2.95	2.4	2.86

An inverse analysis is applied to determine the tensile model parameters (k_y, f_t, and f_y) for this structure. More specifically, the load-deflection output was obtained from finite element analysis with different sets of tensile strength parameters until a "Best Fit" set of values was achieved for the tensile model parameters. All the other input parameters (Table 1), the ductility ratio $k_y/f_t = 10$, and the stiffness ratio $K_1/K_0 = 3\%$ (Figure 1) were presumed to stay constant (as required by a size independent ductility ratio as described by Chuang & Ulm, 2002a).

Figure 5 (b) (labeled "Best Fit") shows the FE load-deflection prediction for SS4P using $\Sigma_1^- = k_y + f_t = 10.5$ MPa, $\Sigma_1^+ \approx k_y = 9.6$ MPa, and $\Sigma_2 = k_y + f_y = 12.5$ MPa (for details, refer to Table 2), which shows very good correlation with the experimental result. As expected, the first cracking strength Σ_1^- and the post-cracking strength Σ_1^+ for the small scale test are significantly higher (38% higher than the "Original" values, $\Sigma_1^- = 7.6$ MPa and $\Sigma_1^+ = 6.9$ MPa) than those of the large scale test due to size effects. By contrast, the change to the composite yield strength Σ_2 is insignificant (less than 9%). Furthermore, using the same ductility ratio k_y/f_t and stiffness ratio K_1/K_0, a very consistent load-deflection prediction is achieved. These result appears to confirm the size dependence of parameters k_y and f_t, but also the size independence of the ductility ratio k_y/f_t. Despite size dependent first cracking and post-cracking strengths, the ductility (the ductility ratio, the stiffness ratio and the composite yield strength) is shown to be size independent.

4.2 Size Effect Study on Self-Similar Small Scale Notched Beams

Precise evaluation of size effects entails the investigation of the strength behavior of geometrically self-similar structures (e.g. Bažant & Planas, 1998). For this purpose, two self-similar notched three-point bending tests performed by Lafarge are considered. The smaller beam (N70) had a total test span of L = 210 mm, a height of h = 70 mm, a width of b = 70 mm, and an initial crack height a = 7 mm. The larger beam (N100) had a total test span of L = 300 mm, a height of h = 100 mm, a width of b = 100 mm, and an initial crack height a = 10 mm. For both tests, the initial crack width was estimated to be 2 mm. While the self-similarity ratio for both structures is small, $h_{N100}/h_{N70} = 1.43$, the tests still exemplify potential size effects on UHPC.
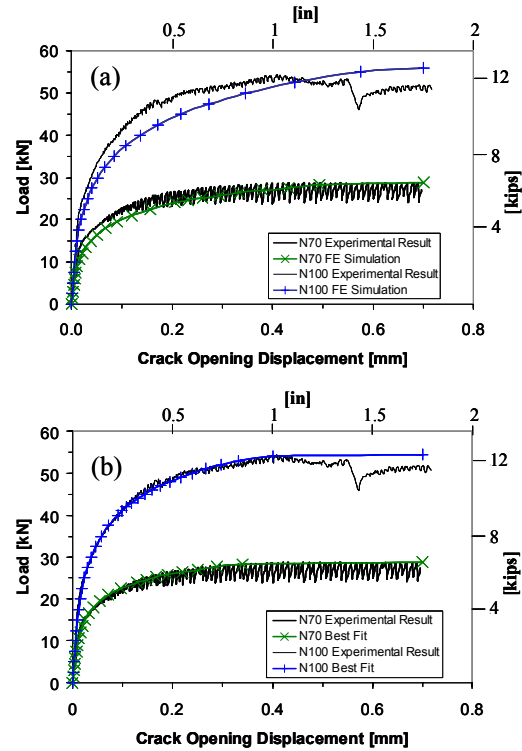

Figure 6: Total load as a function of crack opening displacement as given by the experimental data and FE simulation for (a) "Original" material parameters and (b) "Best Fit" material parameters.

Figure 6(a) shows the total load P as a function of crack opening displacement for both beams. The crack opening displacement, which is initialized at zero, is measured at the bottom of the beam at a gauge length of 40 mm with a special yoke designed for this purpose (Chanvillard, 2002). Figure 6(a) also presents the FE simulations for both beams using the original UHPC material parameters ("Original" values in Table 2). As expected, the "Original" material parameters underestimate the actual material response in this small scale notched configuration. This underestimation manifests itself at lower loads, particularly near the onset of plasticity. This can be associated with an insufficient first cracking strength value in the simulation.

Trial and error style inverse analyses were employed to determine the tensile model parameters (k_y, f_t, and f_y) for each notched beam test. As in the SS4P simulation, all the other model parameters (Table 1), the stiffness ratio K_1/K_0, and the ductility ratio k_y/f_t were not changed. The "Best Fit" results from the inverse analyses for both notched beams are plotted in Figure 2(b). For N100, $\Sigma_1^- = k_y + f_t = 9.5$ MPa, $\Sigma_1^+ \approx k_y = 9.1$ MPa, and $\Sigma_2 = k_y + f_y = 11.5$ MPa; for N70, $\Sigma_1^- = k_y + f_t = 10$ MPa, $\Sigma_1^+ \approx k_y = 8.6$ MPa, and $\Sigma_2 = k_y + f_y = 11.5$ MPa (see Table 2 for details).

As expected, both beams display higher first cracking strengths Σ_1^- and post-cracking strengths Σ_1^+ than originally determined for the "Original" data. In addition, the larger notched beam, N100, exhibits lower first cracking and post-cracking strengths than the smaller notched beam, N70. Furthermore, the composite yield strengths for both notched tests are identical to the original composite yield strength. For these small scale notched tests, the first cracking strength and the post-cracking strength are size dependent, while the ductility (ductility ratio, stiffness ratio, and composite yield strength) is size independent.

4.3 Interpretation of Results with Bažant's Size Effect Law

Bažant proposes a size effect law, which one can use to estimate the first cracking strength $\Sigma_1^{-,est}$ and post-cracking strength $\Sigma_1^{+,est}$ at different structural scales (Bažant & Planas, 1998):

$$\Sigma_1^{-,est} = \frac{B^- \Sigma_1^{-,ref}}{\sqrt{1 + D/D_0^-}} \qquad (1)$$

$$\Sigma_1^{-,est} = \frac{B^+ \Sigma_1^{+,ref}}{\sqrt{1 + D/D_0^+}} \qquad (2)$$

where $\Sigma_1^{-,ref}$ and $\Sigma_1^{+,ref}$ are reference first cracking and post-cracking strengths. D (dimension [D] = L) is the characteristic size of the structure in question. B (dimensionless) and D_0 (dimension $[D_0]$ = L) are constants (for both the first cracking and post-cracking estimates -/+) which depend on the fracture properties of the material and on the geometry of the structure, but are size independent. That is, B and D_0 are constants for self-similar structures. Bažant's size effect equation bridges the asymptotic solutions of strength theories, which govern the cracking strength of small structures $D/D_0 < 1$, and fracture theories, which govern large structures $D/D_0 > 1$. For very large scale structures, $D/D_0 \gg 1$, Bažant's size effect equation asymptotically approaches the $[D]^{-1/2}$ size dependency of the cracking strength parameters f_t and k_y (Chuang & Ulm, 2002b).

With the data supplied by the N70 and N100 tests, one may calculate the size effect parameters B and D_0 from Equations (1) and (2). For the UHPC material and this notched beam geometry for N70 and N100 where D = h is the height of the beam, the size effect constants are: $\Sigma_1^{-,ref}$ = 7.6 MPa, B^- = 1.52, D_0^- = 207.8 mm; $\Sigma_1^{+,ref}$ = 6.9 MPa, B^- = 1.49, D_0^+ = 249.0 mm. The normalized size affected cracking stresses ($\Sigma_1^{-,est}/B^- \Sigma_1^{-,ref}$ and $\Sigma_1^{+,est}/B^+ \Sigma_1^{+,ref}$) are plotted in Figure 7 as a function of the normalized heights of the notched beam (D/D_0^- and D/D_0^+) as determined from (1) and (2) which are calibrated with the N70 and N100 tests.
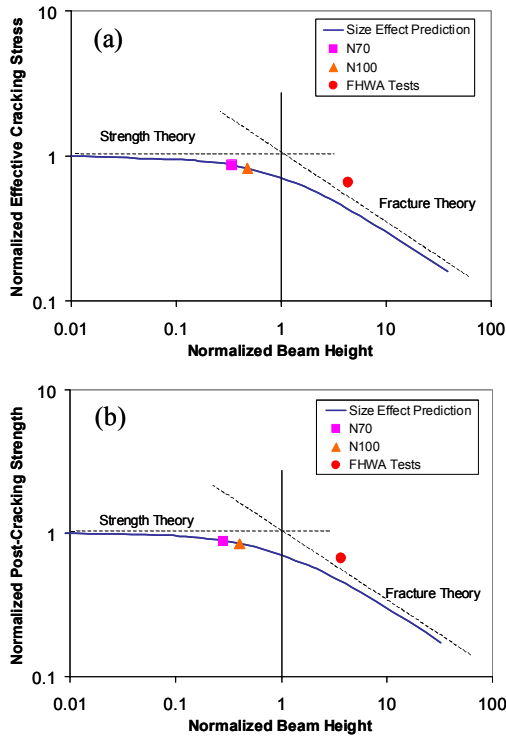
Figure 7: Bažant's size effect prediction shown with N70, N100, and FHWA cracking strength results: (a) Normalized effective first cracking strength as a function of normalized beam height; (b) Normalized effective post-cracking strength as a function of normalized beam height.

Data points obtained from the FHWA tests ($\Sigma_1^{-,\text{est}}$ = 7.6 MPa, h/D_0^- = 4.4) and ($\Sigma_1^{+,\text{est}}$ = 6.9 MPa, h/D_0^+ = 3.7)) are also graphed in Figure 7. As demonstrated, the FHWA test data point lie above the size effect predictions. The size effect predictions for the FHWA tests given by Bažant's law are $\Sigma_1^{-,\text{est}}$ (D = 910 mm) = 5.0 MPa and $\Sigma_1^{+,\text{est}}$ (D = 910 mm) = 4.8 MPa. This discrepancy may stem from two possible sources:

- The size effect parameters only apply to UHPC in this particular notched geometry. Accordingly, underestimation of the effective strength $\Sigma_1^{-,\text{est}}$ given by Bažant's equation is likely due to the notch effect which imposes stress intensities which induce cracking at lower loads.
- Additionally, this discrepancy may be due to the insufficiency of two data points (from N70 and N100) to provide precise values for B and D_0. For example, if the

values of first cracking for the N100 and N70 tests were $\Sigma_1^{-,\text{est}}$ = 9.6 MPa (1% change) and $\Sigma_1^{-,\text{est}}$ = 9.8 MPa (2% change), respectively, the newly calibrated size effect law would provide a value of $\Sigma_1^{-,\text{est}}$ (D=910 mm) = 6.6 MPa, a 32% change. Clearly, more size effect data is required at different structural scales to provide reliable cracking strength estimations.

5 CONCLUSIONS

The design of the next generation of UHPC structures will undoubtedly utilize the tensile strengths of UHPC in efficient applications. However, this utilization is predicated on the reliability and stability of these tensile strengths. Along with exacting manufacturing and testing processes, as well as strict crack control requirements, the reliability of tensile strengths at different structural scales will be required.

To this end, this report presents an investigation into the size independence of UHPC ductility. Using beam tests in conjunction with UHPC modeling methods and tools, the scaling characteristics of UHPC tensile behavior are investigated. It is shown that the first cracking strength and the post-cracking strength of UHPC materials are indeed size dependent. However, it is revealed that the ductile behavior of UHPC is size independent. More specifically, the ductility ratio at first cracking, the stiffness ratio, and the ultimate strength are all shown to be size independent. It is the size independence of the ultimate strength which will allow for the safe use of UHPC tensile strength in structural design.

6 REFERENCES

Bažant, Z. & Planas, J. 1998. *Fracture and size effect in concrete and other quasibrittle materials* New York: CRC Press.

Chanvillard, G. 2002. Personal communication.

Chuang, E. & Ulm, F.-J. 2002a. *Ductility Enhancement of High Performance Cementitious Composites and Structures*. MIT-

CEE Report R02-02 to the Lafarge Corporation.

Chuang, E. & Ulm, F.-J. 2002b. A Two-Phase Composite Model for High Performance Cementitious Composites and Structures. *Journal of Engineering Mechanics*, ASCE, Vol. 128(12): 1314-1323.

Chuang, E. & Ulm, F.-J. 2003. Ductility enhancement of UHPC materials and structures I. 3-D constitutive model. *Submitted to the ASCE Journal of Engineering Mechanics*.

Chuang, E., Park, H. & Ulm, F.-J. 2003. Ductility enhancement of UHPC materials and structures II. Model based simulation. *Submitted to the ASCE Journal of Engineering Mechanics*.

Federal Highway Administration (FHWA). 2002. U-HPC testing: shear. Handout made available at FHWA shear test.

Park, H., Ulm, F.-J. & Chuang, E. 2003. *Model-based optimization of ultra-high performance concrete highway bridge girders*. MIT-CEE Report R03-01 to the Federal Highway Administration.